DOI: 10.1002/ange.201307339

Self-Replication

Accelerated Self-Replication under Non-Equilibrium, Periodic Energy Delivery**

Rui Zhang, David A. Walker, Bartosz A. Grzybowski, and Monica Olvera de la Cruz**

Abstract: *Self-replication is a remarkable phenomenon in nature that has fascinated scientists for decades. In a self-replicating system, the original units are attracted to a template, which induce their binding. In equilibrium, the energy required to disassemble the newly assembled copy from the mother template is supplied by thermal energy. The possibility of optimizing self-replication was explored by controlling the frequency at which energy is supplied to the system. A model system inspired by a class of light-switchable colloids was considered where light is used to control the interactions. Conditions under which self-replication can be significantly more effective under non-equilibrium, cyclic energy delivery than under equilibrium constant energy conditions were identified. Optimal self-replication does not require constant energy expenditure. Instead, the proper timing at which energy is delivered to the system is an essential controllable parameter to induce high replication rates.*

From DNA to cells to organisms, self-replication is a carefully orchestrated process spanning multiple length scales and ensuring the sustainability of life on Earth. Not surprisingly, self-replication phenomena have been widely studied, not only by biologists, with several remarkable attempts to construct artificial replicators based on mechanical machines[1] or chemical systems.[2] Recently, Seeman and co-workers reported an artificial self-replicating material made from synthetic DNA tile motifs[3] with self-replication driven by multiple chemical and thermal processing cycles, without the use of biological controls, such as enzymes. Although Seeman's system does not yet achieve exponential growth in the population of the replicated species, it points to one of the key, yet often overlooked, characteristics of self-replication systems; namely, the need for energy cycling to bind/unbind the system's components. During self-replication, the monomers have to first assemble onto the template (where they bind to one another), but then must disengage from this template to serve as templates themselves. At equilibrium, such a reversal of interactions can only be facilitated by the random noise of thermal energy, $k_B T$, disrupting the binding between the original template and its assembled copy; even intuitively this scenario is inefficient and, in fact, it is not used in biological system where disassembly is driven by an appropriately synchronized input of chemical energy (for example, DNA helicases powered by ATP separate long DNA strands that would otherwise require temperatures well above biological conditions to melt). Conditions of time-varying energy input necessarily bring us to the realm of non-equilibrium that we consider herein.[4,5] The main question we ask is whether the overall efficiency of self-replication (measured by the rate at which templates are replicated) can be controlled and optimized by the frequency at which energy is supplied to the system. Although the current study is a theoretical one, it is inspired by a recently demonstrated class of colloids in which, the assembly/disassembly can be driven by external impulses, including light.[5,6] In the specific model we consider herein, particle dimers replicate from particle monomers with the interactions between all of these species toggled between attractive and repulsive by external pulses of (light) energy. Based on extensive computer simulations, we demonstrate that the exponential growth rates of this self-replicating system can be significantly enhanced by delivering the energy pulses at specific frequencies. To the best of our knowledge, this is the first indication (naturally, to be verified in future experiments) that the rate of self-replication can be controlled by the periodicity of external stimuli. In other words, optimal self-replication does not necessarily require constant energetic expenditure; instead what matters is the proper timing with which energy is delivered to the system.

Our model self-replicating system is illustrated in Figure 1. Initially, in the absence of light, this system comprises a template (T, a dimer of particles) and a collection of individual particles, P, all of which are weakly repulsive by the so-called Weeks–Chandler–Andersen (WCA) potential.[7] When light is turned on (the ON state), the interactions between the dimer and between all particles become attractive, as prescribed by the Lennard-Jones (LJ) pairwise

[*] Dr. R. Zhang, Prof. M. Olvera de la Cruz
Department of Materials Science and Engineering
Northwestern University, Evanston, IL (USA)
D. A. Walker, Prof. B. A. Grzybowski, Prof. M. Olvera de la Cruz
Department of Chemical and Biological Engineering
Northwestern University, Evanston, IL (USA)
Prof. B. A. Grzybowski, Prof. M. Olvera de la Cruz
Department of Chemistry
Northwestern University, Evanston, IL (USA)
E-mail: grzybor@northwestern.edu
m-olvera@northwestern.edu

[**] We thank Prateek Jha and Vladimir Kuzovkov for stimulating discussions during development of the model. Numerical simulations were performed using the Northwestern University High Performance Computing Cluster Quest. This work was supported by the Non-Equilibrium Energy Research Center (NERC), which is an Energy Frontier Research Center funded by the U.S. Department of Energy, Office of Science, Office of Basic Energy Sciences under Award Number DE-SC0000989. D.A.W. thanks the fellowship from the Northwestern University Materials Research Science and Engineering Center (NU-MRSEC) funded by the NSF under Award Number DMR-1121262.

Supporting information for this article is available on the WWW under http://dx.doi.org/10.1002/anie.201307339.

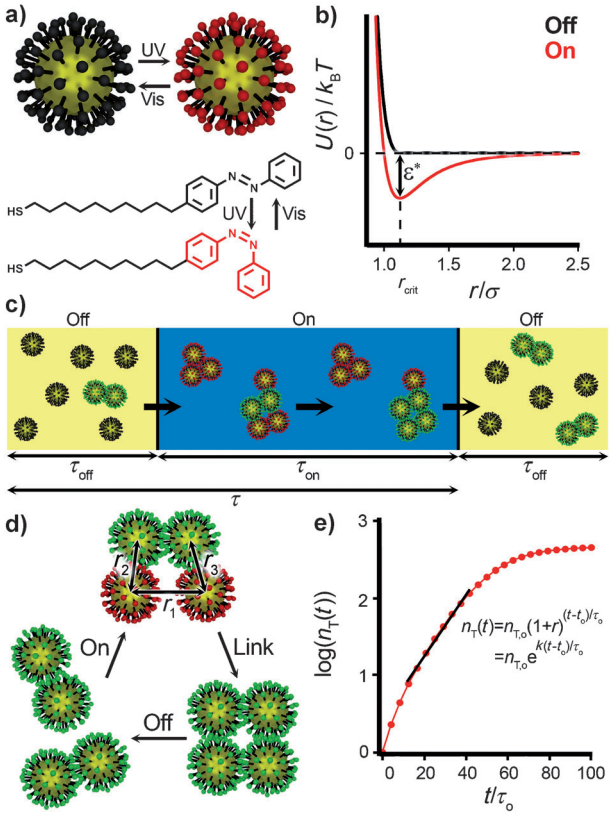

Figure 1. A self-replicating system driven by time-varying energy inputs. a) Our system is inspired by experiments with photoswitchable Au NPs covered with azobenzene-terminated thiols. b) Such systems have been shown to assemble upon irradiation with UV light (ON state) when the azobenzenes develop dipole moments and can interact by attractive dipole–dipole interactions. In the absence of UV irradiation (OFF state), azobenzenes reisomerize into the non-interacting *trans* form. c) Template dimers (show in green) have the ability to bind monomers (shown in red) and cross-link them to form new daughter templates. The periodic light/energy input (and thus the alternating interparticle interactions) sequence is fully described by the variables τ/τ_0, where $\tau=\tau_{on}+\tau_{off}$ is the period and τ_{on}/τ is the fraction of the period in which the attractive interactions are ON. d) Representation of the self-replication process. e) Typical growth kinetics of dimers from monomers; the exponential growth phase of the kinetic profile typically resides between $n_T=10$–100 dimers (corresponding to black fit line), which can be characterized by either an exponential growth rate r or exponential growth constant k.

potentials (for experimental realization, see Refs. [5,8]). The strength of the attraction is quantified by the depth of the attraction well ε (the dimensionless parameter $\varepsilon^*=\varepsilon/k_B T$ is used in the following discussion, where k_B is the Boltzmann constant and T is absolute temperature). If two individual particles and a dimer template move close to one another such that the three interparticle distances r_1, r_2, and r_3 (Figure 1d) are all smaller than a critical distance r_{crit} (typically, $2^{1/6}\sigma$, where σ is the diameter of the particles), the two spheres immediately bind to form a new dimer in a reaction $T+2P\rightarrow 2T$. When the light is turned off (OFF state), the interactions between all entities become weakly repulsive and the newly formed daughter templates can disassemble from the original mother templates. In this way, the mother templates self-replicate and in subsequent cycles can promote the formation of more daughter templates from individual nanoparticles (NPs). In the simulations, we assume the light response of these particles is instantaneous, which, incidentally, is a reasonable assumption to model dilute solutions of the experimentally studied azobenzene-covered, photoswitchable nanoparticles.[5,8]

With these definitions, we implemented the kinetic Monte Carlo (KMC[9–11]) algorithm in a cubic box with periodic boundary conditions to study the dynamics of an ensemble initially comprising n_T templates and n_P individual particles. In a typical run, the total number of spherical units simulated was $n=2n_T+n_P=1000$ with only one template present at time $t=0$. The (dimensionless) particle density is given by $\eta=n\sigma^3 V$, where V is the size of the simulation box. The progress of self-replication was monitored by the number of dimeric templates $n_T(t)$ present at time t. Self-replication was driven by energy pulses of duration τ_{on} followed by times τ_{off} when no energy was delivered (Figure 1c). The parameters we used to describe a pulse sequence were the period $\tau=\tau_{on}+\tau_{off}$, and the ratio τ_{on}/τ (henceforth, referred to as "on-ratio"; note that $\tau_{on}/\tau=1$ when energy is continuously delivered). For each ε^*, η, τ/τ_0, and τ_{on}/τ condition we considered, 100 independent KMC simulations were performed, each starting from randomly chosen particle positions, to give the averaged results we discuss below (see the Methods Section and the Supporting Information for more simulation details).

We first consider a limiting case, $\tau_{on}/\tau=1$, which corresponds to an equilibrium situation of inter-particle interactions not changing and being always attractive. Figure 2a shows the number of templates, $n_T(t)$, semi-logarithmic scale as a function of time for different ε^* values and at the density of $\eta=0.008$; Figure 2c–e provides representative simulation snapshots.

Remarkably, the rates of dimer production exhibit a non-monotonic dependence on the strength of interparticle interactions, ε^*. For strong interactions, $\varepsilon^*\geq 2$, the initial rates of dimer formation are high, but the newly formed dimers cannot easily disengage from the mother ones, resulting in the formation of large aggregates (Figure 2c). As the diffusion of these large clusters is slower than that of individual particles, the probability that particles within a cluster would meet a template (in another cluster) is low, and the process of self-replication rapidly slows to a near halt (see the Supporting Information, Movie S1, for a typical simulation run for $\varepsilon^*=5$ whereby large clusters fuse and particles can replicate only at long times). The situation is markedly different in the weak-interaction regime (for example, $\varepsilon^*=0.7$ curve and Figure 2e snapshot), whereby the newly formed dimers can easily disengage from the templates and can follow an exponential kinetics of dimer production. In this regime, however, the individual particles reside on the dimers only fleetingly, thus lowering the probability of two particles being found on a template simultaneously (and bonding into a new dimer). The most efficient self-replication is observed between the above described regimes, when the interactions are strong enough to hold the template–particle intermediates for longer times yet weak enough to allow for their disassembly by the thermal

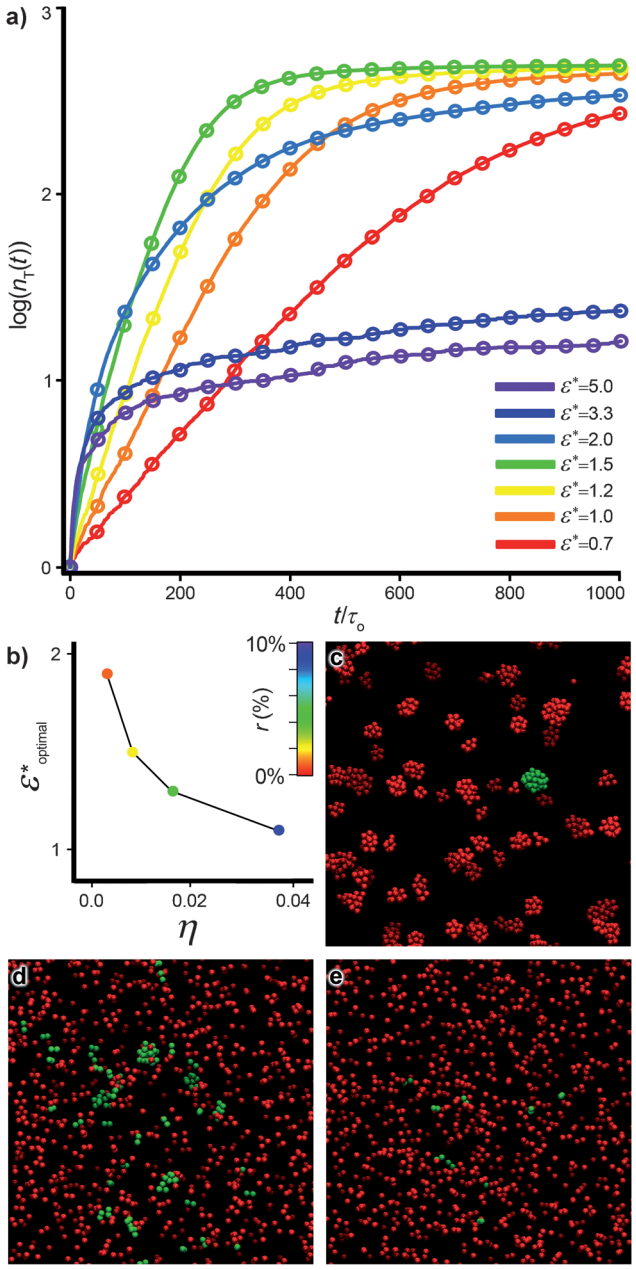

Figure 2. Self-replication under equilibrium conditions. In the scenario of interactions being continuously attractive, desorption of new daughter templates is significantly influenced by the magnitude of the attraction potential ε^*. a) This is clearly observed by monitoring the number of templates $n_T(t)$ in the system as a function of time and ε^*. Here $\eta = 0.008$ (we observe similar trends for all values of η) and $\tau_{on}/\tau = 1$. The plots represent simulations of 1000 particles (that is, maximum $n_T = 500$) averaged over 100 simulations. b) The optimal values of ε^* under continuous energy delivery at varying values of η. c)–e) Typical snapshots ($\eta = 0.008$, $t = 150\,\tau_0$) from the simulations reveal three distinct regimes: c) when the interaction potentials are stronger than thermal noise ($\varepsilon^* = 5$), the conversion is diffusion-limited; d) when the interaction potentials are commensurate with thermal noise ($\varepsilon^* = 1.5$), the monomers are able to adsorb onto and desorb off the templates; e) when the interaction potentials are weak ($\varepsilon^* = 1$), thermal noise dominates the system and the probability that a template will co-localize two monomers is low.

energy. In such an intermediate-strength regime, $\varepsilon^* \approx 1.5$ (see Figure 2d snapshot and Supporting Information, Movie S2), the exponential growth can continue for relatively long times while ensuring the fastest possible conversion of all particles into dimers. Similar trends are observed for different densities (we tested $\eta = 0.003$, 0.008, 0.016, and 0.037) apart from the fact that as η increases, the strength of inter-particle interactions ε^* that yields the fastest rate of self-replication decreases (see Figure 2b). These variations, however, are modest and the ε^* values always remain in a narrow range of about 1–2 $k_B T$ (Supporting Information, Section S1). The general conclusion is, therefore, that under conditions of constant energy, replication is the fastest when the magnitude of attractive interactions between the particles is similar to the thermal noise that tries to break these forming aggregates apart.

The equilibrium case discussed above provides a benchmark for self-replication under non-equilibrium conditions of pulsed energy inputs, $\tau_{on}/\tau < 1$. Figure 3 summarizes the results of simulations spanning a wide parameter space across the four variables defining our system (ε^*, η, τ/τ_0, and τ_{on}/τ). There are two distinct regions in the phase space (Supporting Information, Sections S1–S4). In the first region, observed for larger τ_{on}/τ, ε^*, and η values (pink data points in Figure 3a–d), the templates become trapped in large, internally disordered aggregates such that self-replication is limited by the diffusion and exchange of particles between these large clusters. Under these conditions, the production dynamics never enters an exponential growth phase (for a typical $n_T(t)$ curve in the Supporting Information, Figure S3a). In sharp contrast, in the phase space region corresponding to the blue data points in Figure 3a–d, the aggregates can fully disintegrate and mix in-between light pulses; self-replication is kinetically controlled by the number of remaining monomers, and all template production profiles contain an exponential growth phase (for a typical $n_T(t)$ curve, see the Supporting Information, Figure S3b). To illustrate these features further, Figure 3e–h provide typical snapshots from simulations just before light is turned on (such that the particles are in their most dispersed state; Figure 3e,f) and just before it is turned off (such that the particles are in their most aggregated state; Figure 3g,h). As seen, under the conditions of diffusion limited replication (Figure 3e,g; pink), the aggregates do not have enough time between light pulses to fully disintegrate and, as such, rarely exchange particles between the clusters (Supporting Information, Movie S3). For the kinetically controlled scenario (Figure 3f,h; blue), the smaller aggregates can fully break apart, and the exchange of particles is relatively rapid in comparison to the diffusion-limited scenario (Supporting Information, Movie S4).

With the above understanding of the phase-space of the system, we systematically varied the parameters of our system and calculated (Supporting Information, Section S3) the exponential growth constants, k, for each profile within the kinetically controlled domain (as discussed above and shown in Figure 3). The equation describing the exponential growth regime is $n_T(t) = n_{T,o}\exp(k(t-t_0)/\tau_0)$, where it is convenient to define $1 + r = \exp(k)$ such that r gives the percentage increase in the population per unit time (Figure 1e). The results from

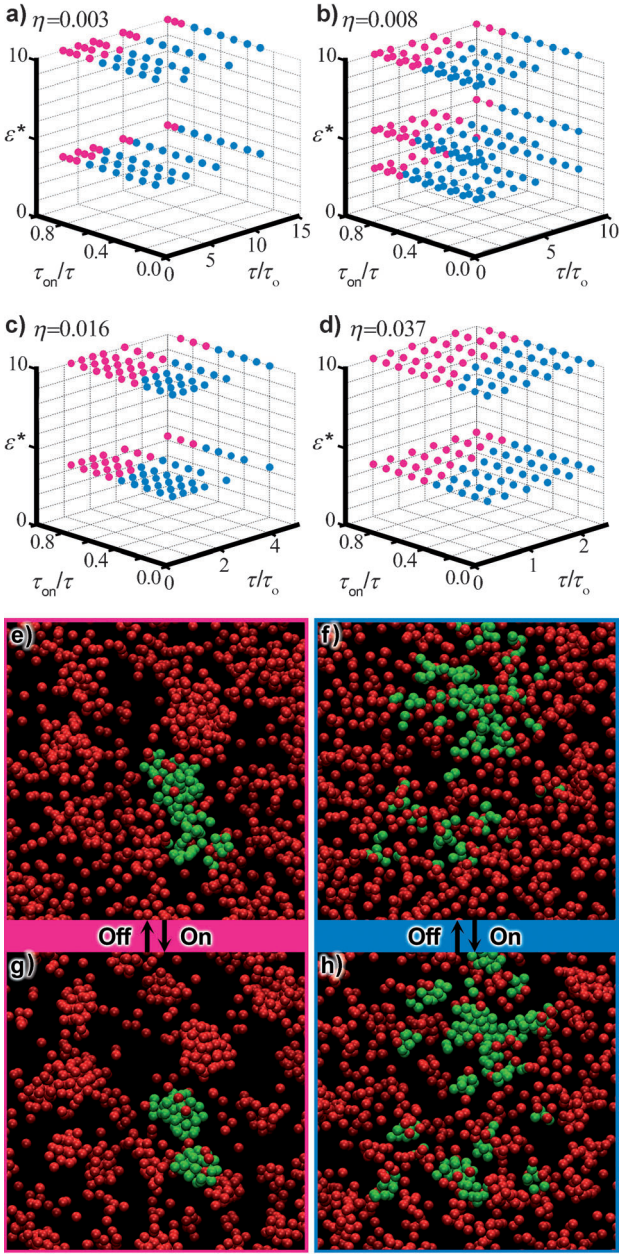

Figure 3. Kinetic phase diagrams for non-equilibrium self-replication. a)–d) Phase diagrams summarizing the dynamics of the pulsed-energy system feature diffusion controlled (pink) or kinetically controlled (blue) regions for a given set of parameters (η, ε^*, τ_{on}/τ, and τ/τ_0). e)–h) Typical snapshots from the simulations illustrate the differences between the diffusion limited parameter space (e,g) and the kinetically limited parameter space (f,h) where exponential growth can occur.

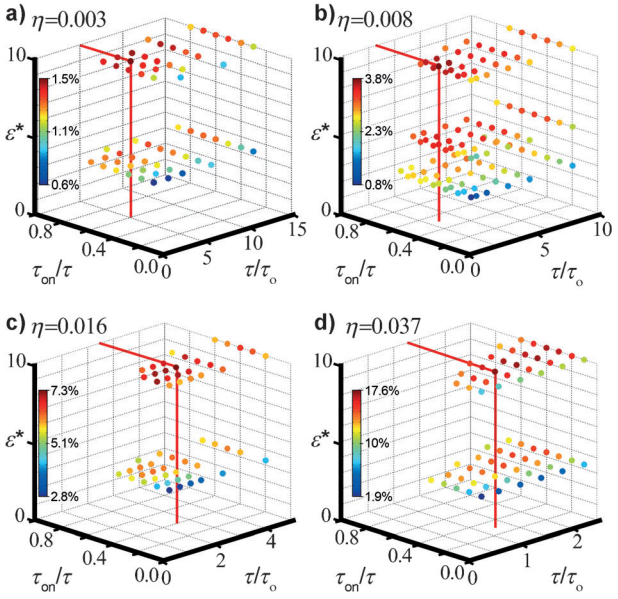

Figure 4. Optimization of exponential self-replication rates. The exponential growth rates r as indicated by the color-scale legends can be optimized by tuning the pulse parameters (τ_{on}/τ and τ/τ_0) for multiple interaction potentials (ε^*) and densities; here a) $\eta = 0.003$, b) $\eta = 0.008$, c) $\eta = 0.016$, and d) $\eta = 0.037$. The maximal values in each plot are delineated by red guidelines to help illustrate how the value changes in the phase space for varying densities.

these simulations are summarized in Figure 4, where the color maps indicate the magnitudes of r values. The most important finding of our work is that for strong inter-particle interactions (Figure 4) there exists a range of energy pulses (defined by the parameters τ/τ_0 and τ_{on}/τ) in which the exponential growth rate is higher than the optimized rate under constant energy (as discussed in Figure 2). For example, when the particle density is $\eta = 0.037$ (see the Supporting Information, Section S2 for discussion of other densities) the optimal/highest possible exponential growth rate for the constant-energy case is $r = 9.5\,\%$ when $\varepsilon^* = 1.1$. In contrast, when energy is delivered in optimized pulsed sequences, an exponential growth rate of $r = 17.6\,\%$ can be achieved when $\varepsilon^* = 10$, which is an 85 % increase in the production rate for the non-equilibrium system as compared to the maximal achievable production rate in the equilibrium system. We note that while the optimized growth rate continues to increase for stronger inter-particle interactions or larger densities (Figure 4), such system parameters become unrealistic in their implementation (that is, interaction potentials become stronger than can be achieved in experiments, the periodicity of light pulsing energy becomes smaller than the kinetic time scales of typical molecular switches; packing densities are too high to allow the crystals to sufficiently melt, and so on).

In conclusion, our theoretical considerations suggest that periodic energy delivery to a self-replicating system can increase the rate of self-replication. To develop efficient self-replicating systems, proper timing of energy delivery outside of the confines of thermodynamic equilibrium should be considered. Of course, construction of such systems in the laboratory remains an exciting yet formidable challenge for experimental research, which we hope to stimulate and facilitate.

Methods

The interaction between two spherical units that are not in the same dimer template was modeled using shifted-LJ (ON state) or WCA (OFF state) potentials[11] (see Figure 1 b). Both potentials can be

expressed in the form $u(r)=u_{LJ}(r)-u_c, r\le r_c; u(r)=0, r>r_c$, where $u_{LJ}(r)=4\varepsilon[(\sigma/r)^{12}-(\sigma/r)^6]$ and r is the distance between the two spherical units. The cut-off distance r_c was 2.5σ and $2^{1/6}\sigma$ for the ON and OFF states, respectively; The tail correction was $u_c=u_{LJ}(r_c)$. Two spherical units in the same dimer template interacted by a harmonic spring potential $u_{bond}(r)=k_s(r-\sigma)^2/2$, where the spring constant k_s was fixed at $200\,k_B T/\sigma^2$. If two individual particles and a dimer template moved close to one another such that the three interparticle distances (see Figure 1 d for definition) were all smaller than $r_{crit}=2^{1/6}\sigma$ (see Figure 1 b), the two spheres immediately bonded to form a new dimer in which they interacted by the harmonic spring potential defined above.

A recently developed kinetic Monte Carlo (KMC) algorithm[10,11] was implemented to simulate the self-replication process. The algorithm was derived from a renormalization approach in which the Smoluchowski diffusion equations are renormalized to a master equation with transition rates identical to the Glauber definition of transition probabilities.[11] In the present work, an NVT ensemble with periodic boundary conditions was used. One dimer template and 998 individual particles (that is, $n=1000$ spherical units in total) were randomly placed in a cubic box at $t=0$. For subsequent times, one KMC step consisted of the following: 1) randomly picking one spherical unit S; 2) randomly generating a direction in the three-dimensional space and attempting a move of S along this direction with a fixed step size a; 3) calculating the energy change Δu caused by this move and accepting the move with the Glauber definition of transition probability $p=1/[1+\exp(\Delta u/k_B T)]$; 4) if the move was accepted, checking whether the self-replication condition was satisfied, if so, updating the particle type. A KMC sweep contained n such KMC steps and corresponded to a step in time given by $\Delta t=\tau_0(a/\sigma)^2/12$.[11] The step size a was chosen as 0.1σ, consistent with previous KMC simulations in similar light-switchable nanocolloid systems. See Ref. [11] for a justification of this step size and discussion about the advantages of the KMC method over the traditional Brownian dynamics approach. For each set of system parameters studied, 100 independent KMC simulations were performed giving the averages discussed in the main text.

Received: August 21, 2013
Published online: November 15, 2013

Keywords: colloids · kinetic Monte Carlo simulations · light switchable systems · non-equilibrium · self-replication

[1] a) L. S. Penrose, *Sci. Am.* **1959**, *200*, 105 – 114; b) S. Griffith, D. Goldwater, J. M. Jacobson, *Nature* **2005**, *437*, 636 – 636; c) V. Zykov, E. Mytilinaios, B. Adams, H. Lipson, *Nature* **2005**, *435*, 163 – 164.

[2] a) M. Sipper, *Artif. Life* **1998**, *4*, 237 – 257; b) M. E. Leunissen, R. Dreyfus, R. J. Sha, T. Wang, N. C. Seeman, D. J. Pine, P. M. Chaikin, *Soft Matter* **2009**, *5*, 2422 – 2430.

[3] T. Wang, R. Sha, R. Dreyfus, M. E. Leunissen, C. Maass, D. J. Pine, P. M. Chaikin, N. C. Seeman, *Nature* **2011**, *478*, 225 – 228.

[4] a) M. Fialkowski, K. J. M. Bishop, R. Klajn, S. K. Smoukov, C. J. Campbell, B. A. Grzybowski, *J. Phys. Chem. B* **2006**, *110*, 2482 – 2496; b) I. Prigogine, *Étude thermodynamique des phénomènes irréversibles*, Dunod, Paris, **1947**; c) K. V. Tretiakov, I. Szleifer, B. A. Grzybowski, *Angew. Chem.* **2013**, *125*, 10494 – 10498; *Angew. Chem. Int. Ed.* **2013**, *52*, 10304 – 10308.

[5] R. Klajn, K. J. M. Bishop, B. A. Grzybowski, *Proc. Natl. Acad. Sci. USA* **2007**, *104*, 10305 – 10309.

[6] a) J. Palacci, S. Sacanna, A. P. Steinberg, D. J. Pine, P. M. Chaikin, *Science* **2013**, *339*, 936 – 940; b) T. Iida, *J. Phys. Chem. Lett.* **2012**, *3*, 332 – 336.

[7] J. D. Weeks, D. Chandler, H. C. Andersen, *J. Chem. Phys.* **1971**, *54*, 5237 – 5247.

[8] R. Klajn, P. J. Wesson, K. J. M. Bishop, B. A. Grzybowski, *Angew. Chem.* **2009**, *121*, 7169 – 7173; *Angew. Chem. Int. Ed.* **2009**, *48*, 7035 – 7039.

[9] R. Zhang, P. K. Jha, M. Olvera de la Cruz, *Soft Matter* **2013**, *9*, 5042 – 5051.

[10] P. K. Jha, V. Kuzovkov, M. Olvera de la Cruz, *ACS Macro Lett.* **2012**, *1*, 1393 – 1397.

[11] P. K. Jha, V. Kuzovkov, B. A. Grzybowski, M. Olvera de la Cruz, *Soft Matter* **2012**, *8*, 227 – 234.

